iScience, Volume *26*

Supplemental information

Muscle denervation promotes functional interactions between glial and mesenchymal cells through NGFR and NGF

Chiara Nicoletti, Xiuqing Wei, Usue Etxaniz, Chiara D'Ercole, Luca Madaro, Ranjan Perera, and Pier Lorenzo Puri

Supplementary Figure 1

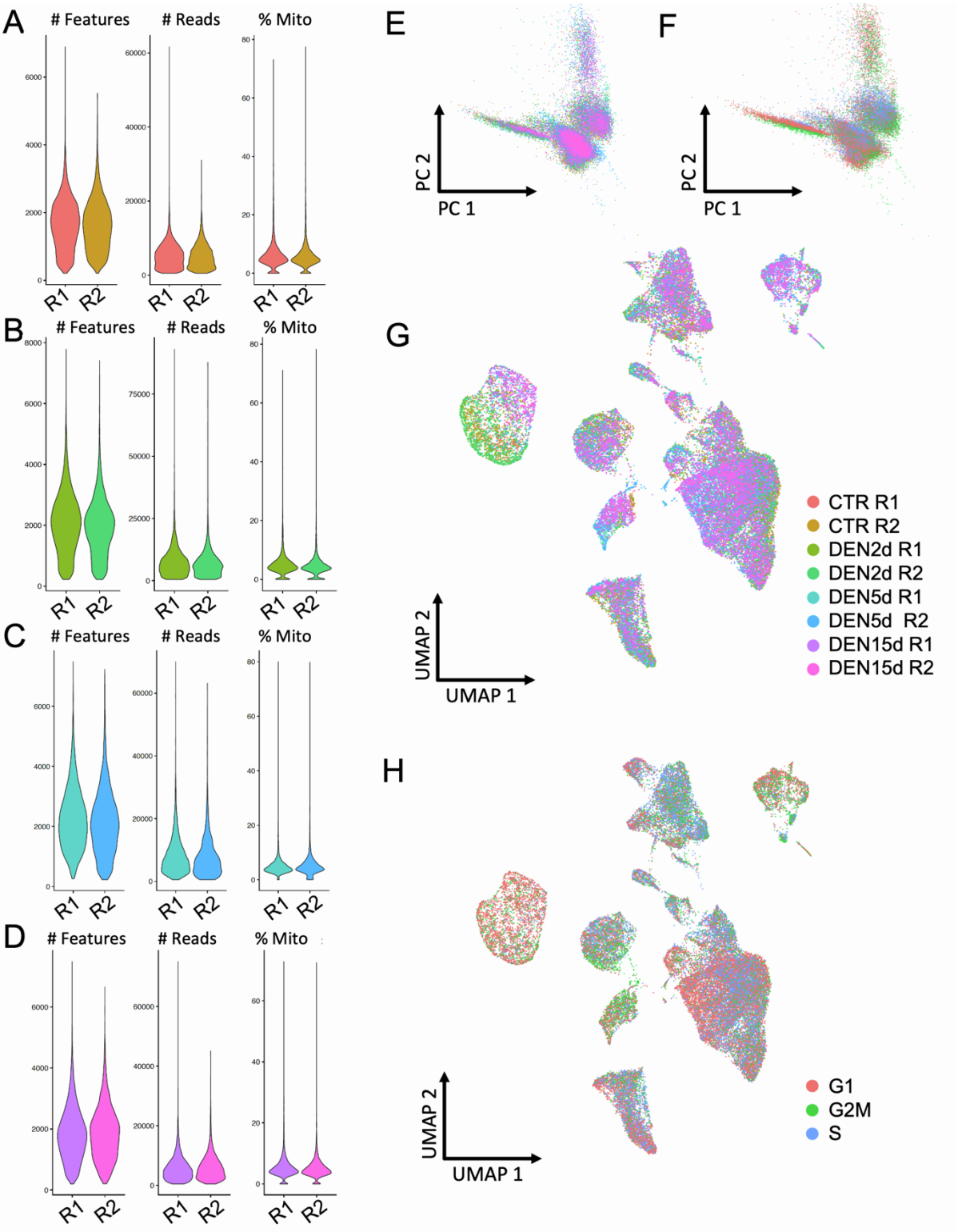

Figure S1. scRNA-seq quality controls and dimensionality reduction, Related to Figure 1

(A-D) Number of genes (# Features), sequencing reads (# Reads) and percentage of mitochondrial transcripts (% Mito) for each cell and each biological sample (R1 and R2) in (A) CTR, (B) 2-days, (C) 5-days and (D) 15-days post-denervation.

(E-F) PCA embedding of all the single cells comprising the dataset colored by either (G) biological replicate or (H) cell cycle phase.

(G) UMAP embedding of all the single cells comprising the dataset colored by biological replicate.

(H) UMAP embedding of all the single cells comprising the dataset colored by cell cycle phase.

Supplementary Figure 2

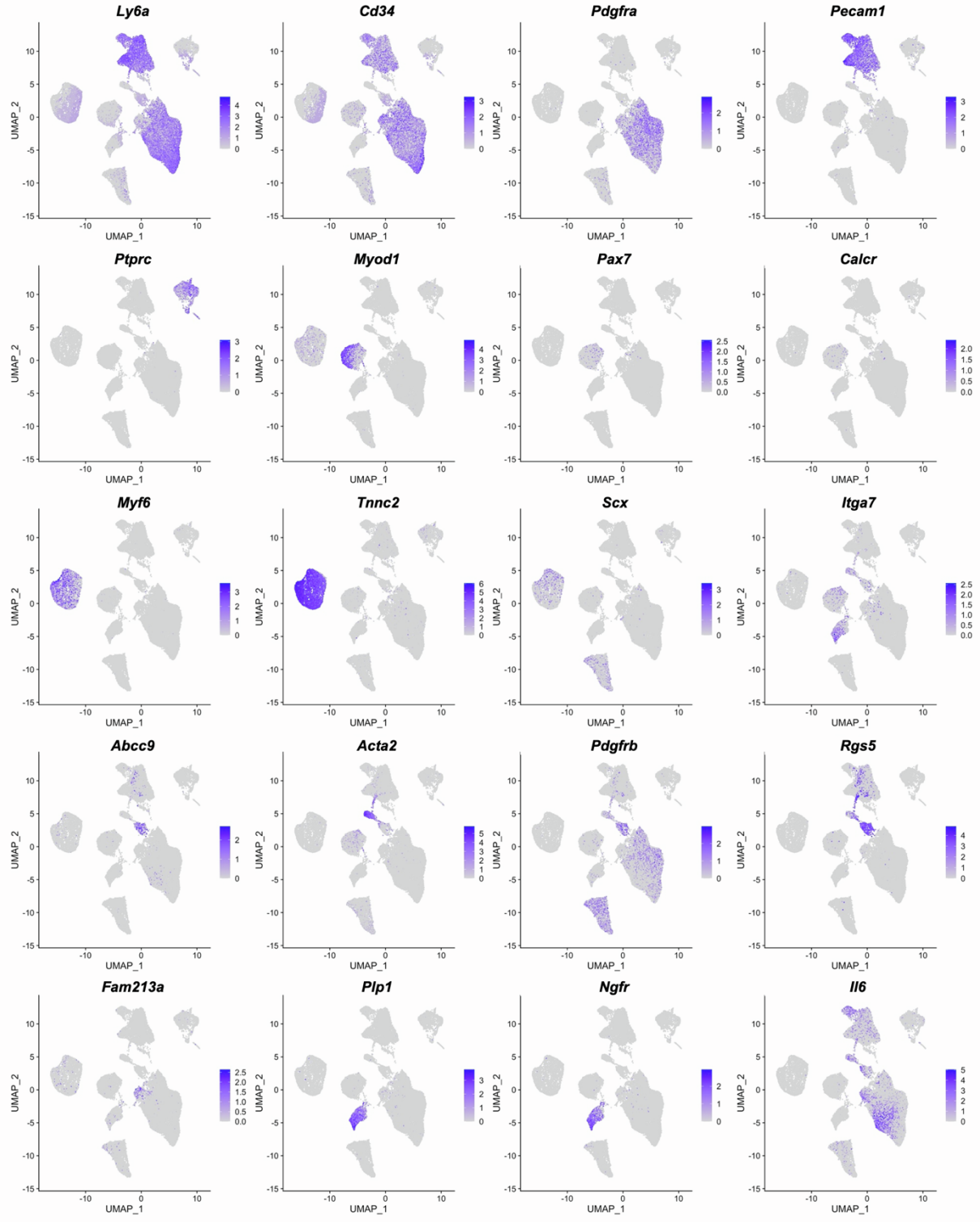

Figure S2. UMAP embedding of cell type-specific genes, Related to Figure 1

UMAP embedding of cell type-specific representative genes in all the single cells.

Supplementary Figure 3

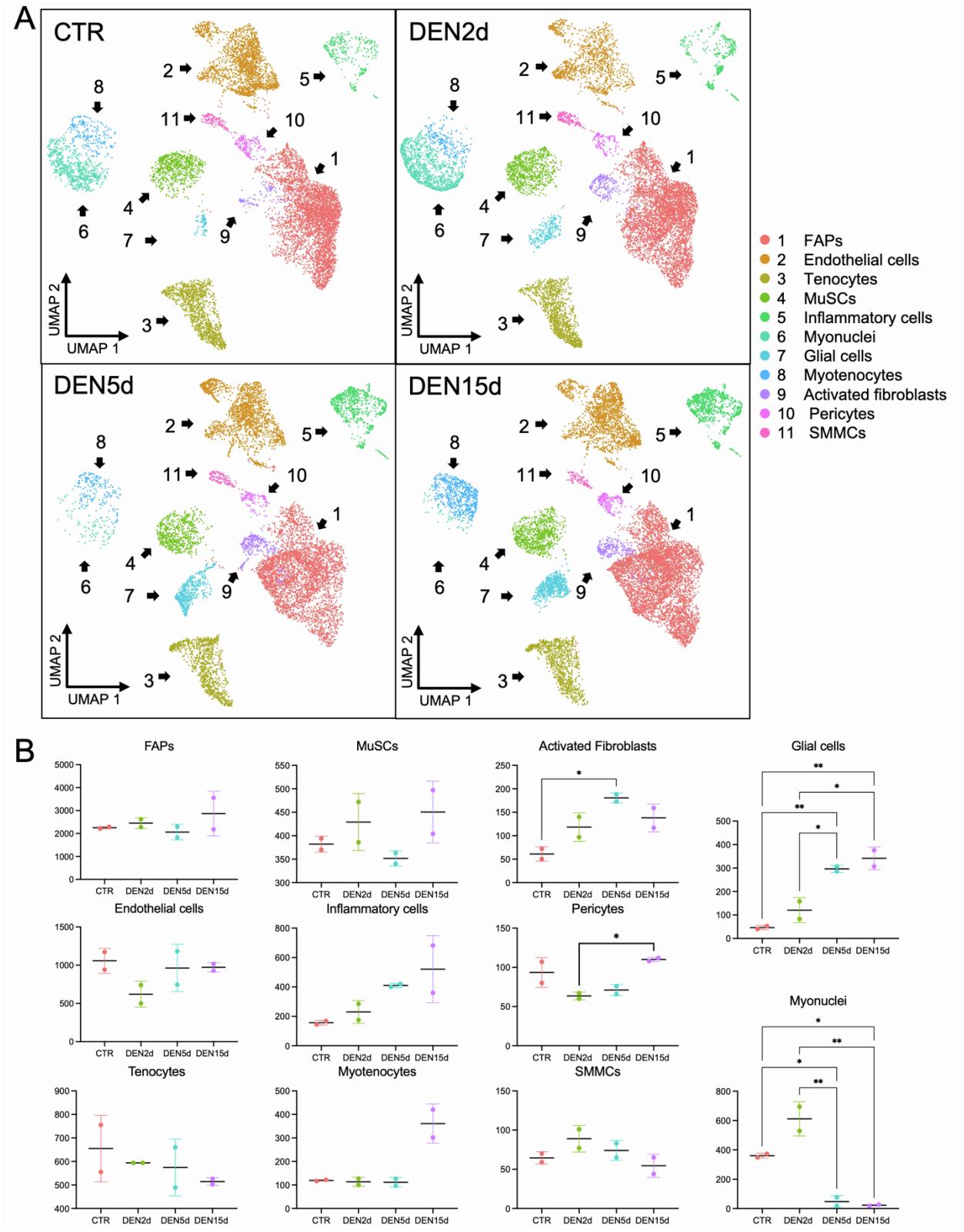

Figure S3. Dynamic changes of muscle-resident cells following denervation, Related to Figure 2

(A) UMAP embedding of single cells at CTR, DEN2d, DEN5d, and DEN15d, respectively. (B) Line plots showing the number of each cell population per condition per replicate. Statistical significance was analyzed by one-way ANOVA with P values shown as *p < 0.05. Not significant P values are not labeled.

Supplementary Figure 4

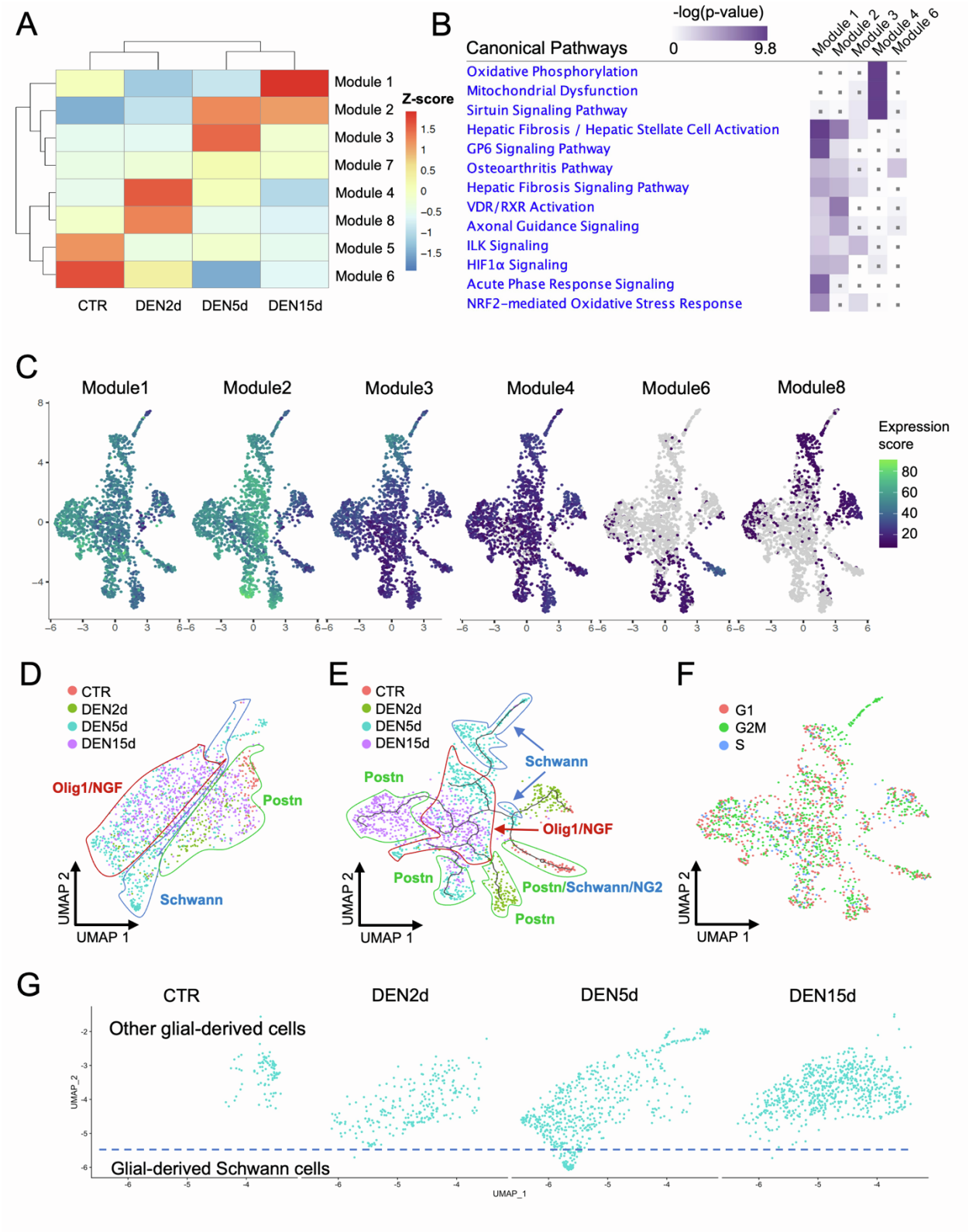

Figure S4. Pseudo-time analysis of glial cells during denervation, Related to Figure 3

(A) Monocle3 module analysis of co-expression of genes found differentially expressed along the pseudo-time trajectory.

(B) IPA analysis of genes belonging to modules enriched at each time point.

(C) UMAP embedding of the enrichment of genes (enrichment score) belonging to the major modules.

(D, E) Same as Figure 3D and 3E, with circles indicating different glial-derived lineages. Red circle: cells expressing *Olig1* and *Ngf*; Green circle: cells expressing *Postn*; Blue circle: cells expressing Schwann cells genes.

(F) UMAP embedding of glial cells after re-clustering, colored by cell cycle phase.

(G) UMAP embedding of glial cells before re-clustering at each time point. Dash line delineates the lower tip of Glial-derived Schwann cells that is specific of day 5 p.d.

Supplementary Figure 5

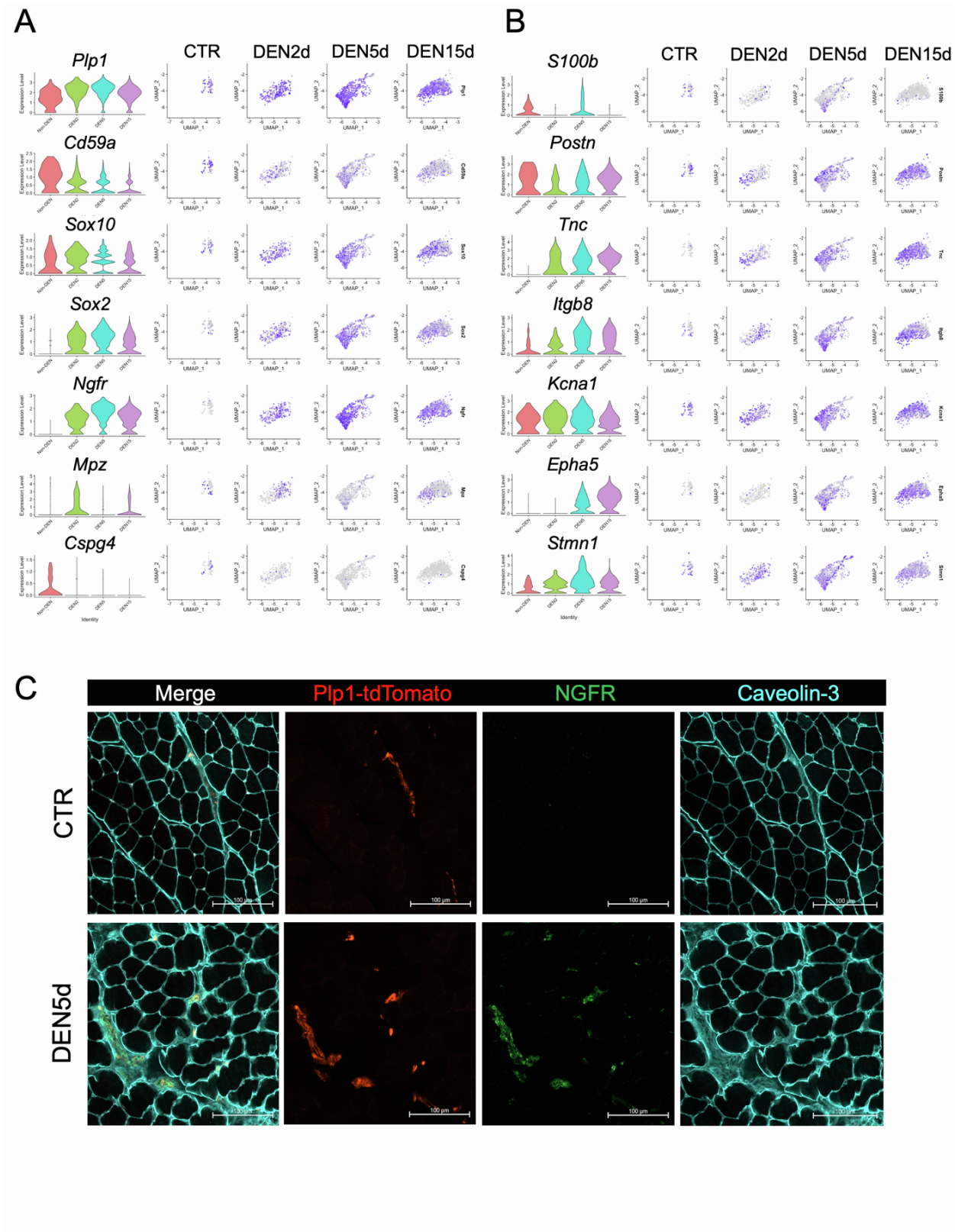

Figure S5. Identification of denervation-activated glial cells, Related to Figure 3

(A-B) Violin (left) and UMAP (right) plots showing dynamic expression of genes of interest in glial cells at each time point.

(C) Representative images of Caveolin-3 (cyan) and NGFR (green) immunofluorescence staining of trans-sectioned TA isolated from Control (CTR, upper) and denervated (DEN5d, lower) *Plp1-TdTomato* (red) mice. NGFR: Nerve Growth Factor Receptor; Plp1: myelin proteolipid protein 1. Scale bar: 100μm. N=4 mice.

Supplementary Figure 6

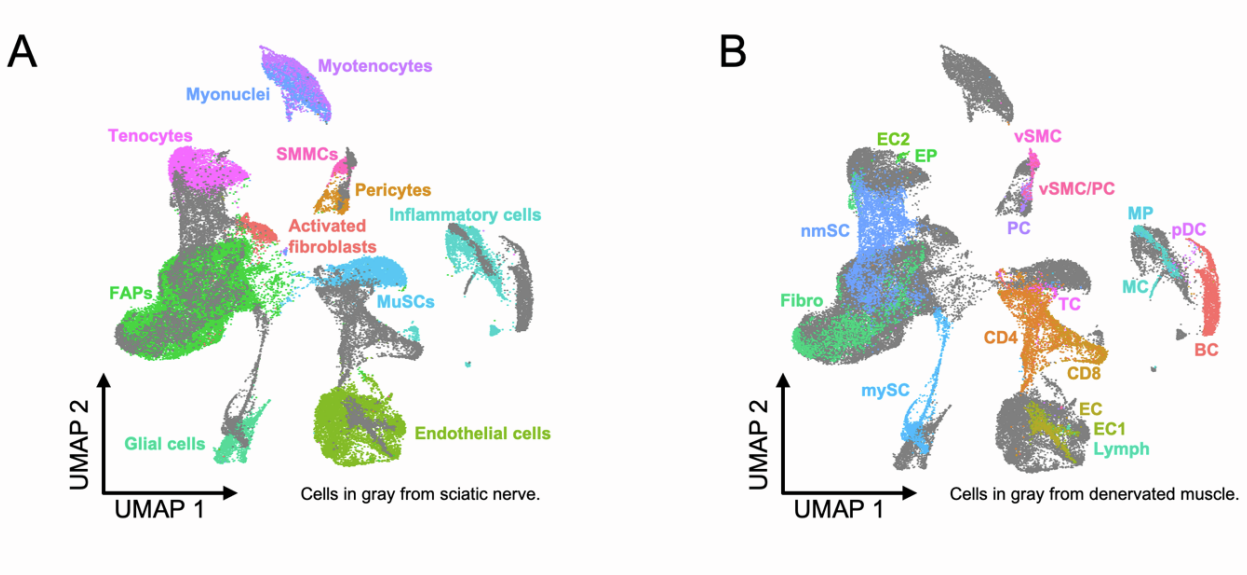

Figure S6. Comparative analysis of denervated muscle and sciatic nerve, Related to Figure 4

(A-B) UMAP embedding of the integration analysis of denervated muscle and sciatic nerve (Wolbert et al., 2020, PNAS) [1], with Wolbert et al. meta-cluster identities (B) or with the meta-cluster identities from our dataset (A).

Supplementary Figure 7

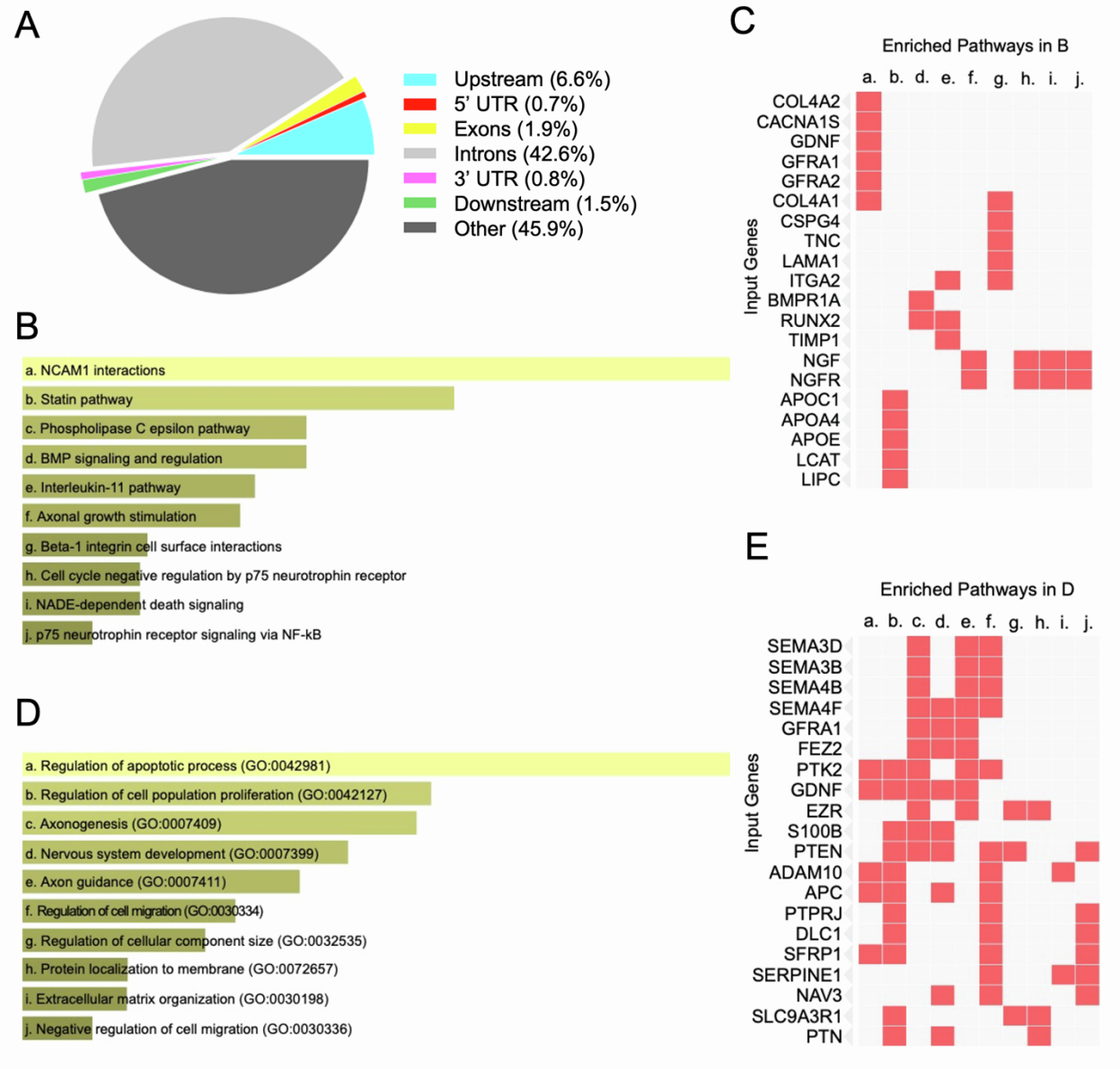

Figure S7. Genomic distribution and gene ontology of differentially accessible regions in muscle-resident cells upon denervation, Related to Figure 5

(A) Pie chart of the distribution of glial cells DARs in relation to genes (Pavis).

(B-E) EnrichR Pathway analysis for glial cells DARs falling either inside promoter regions (B-C; promoters defined as -1000/+200 bp from genes TSS) or non-promoter (D-E, genes used were the glial cells DEGs promoters closest to the non-promoter DARs), with statistically significant pathways ordered by p-value (barplots in B and D). (C) and (E) show a subset of genes related to the DARs and the enriched pathways in (D) and (E), respectively.

Supplementary Figure 8

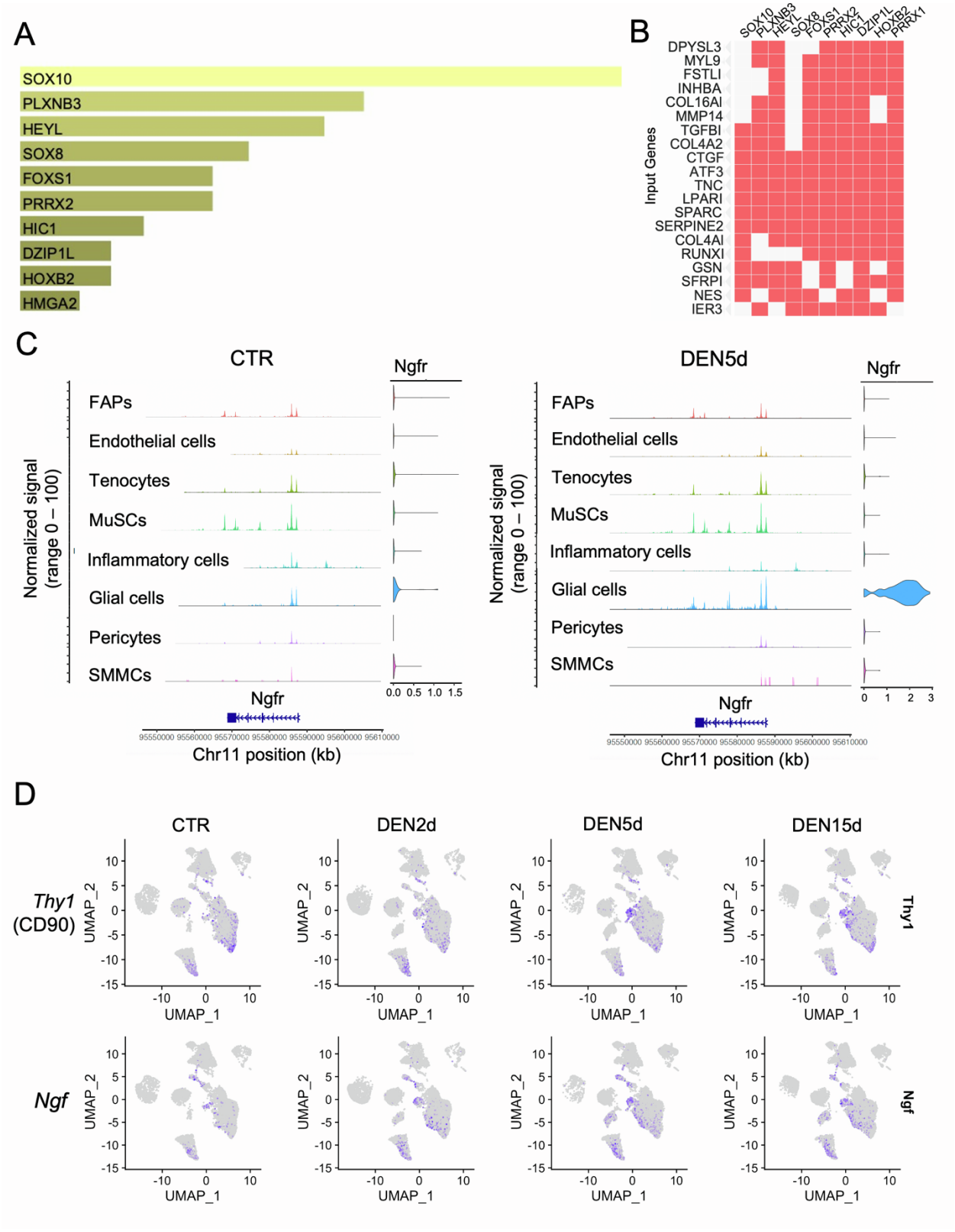

Figure S8. Dynamic chromatin accessibility in muscle-resident glial cells upon denervation, Related to Figure 5

(A-B) EnrichR Submissions TF-Gene Co-occurrence analysis for glial cells DARs falling inside promoter regions (promoters defined as -1000/+200 bp from genes TSS), with statistically significant Transcription Factors ordered by p-value (barplot in A). (B) shows a subset of genes related to the DARs and the enriched Transcription Factors in (A).

(C) Genomic tracks of the cumulative ATAC signal per cell population at the *Ngfr* locus, in control (CTR, left panel) and DEN5d (right panel) conditions. The violin plots of *Ngfr* expression from scRNA-seq data per cell population at CTR and DEN5d are shown on the right of the ATAC signals, respectively.

(D) UMAP embedding of *Thy1* (CD90, upper) and *Ngf* (bottom) in all single cells at each time point.

Supplementary Figure 9

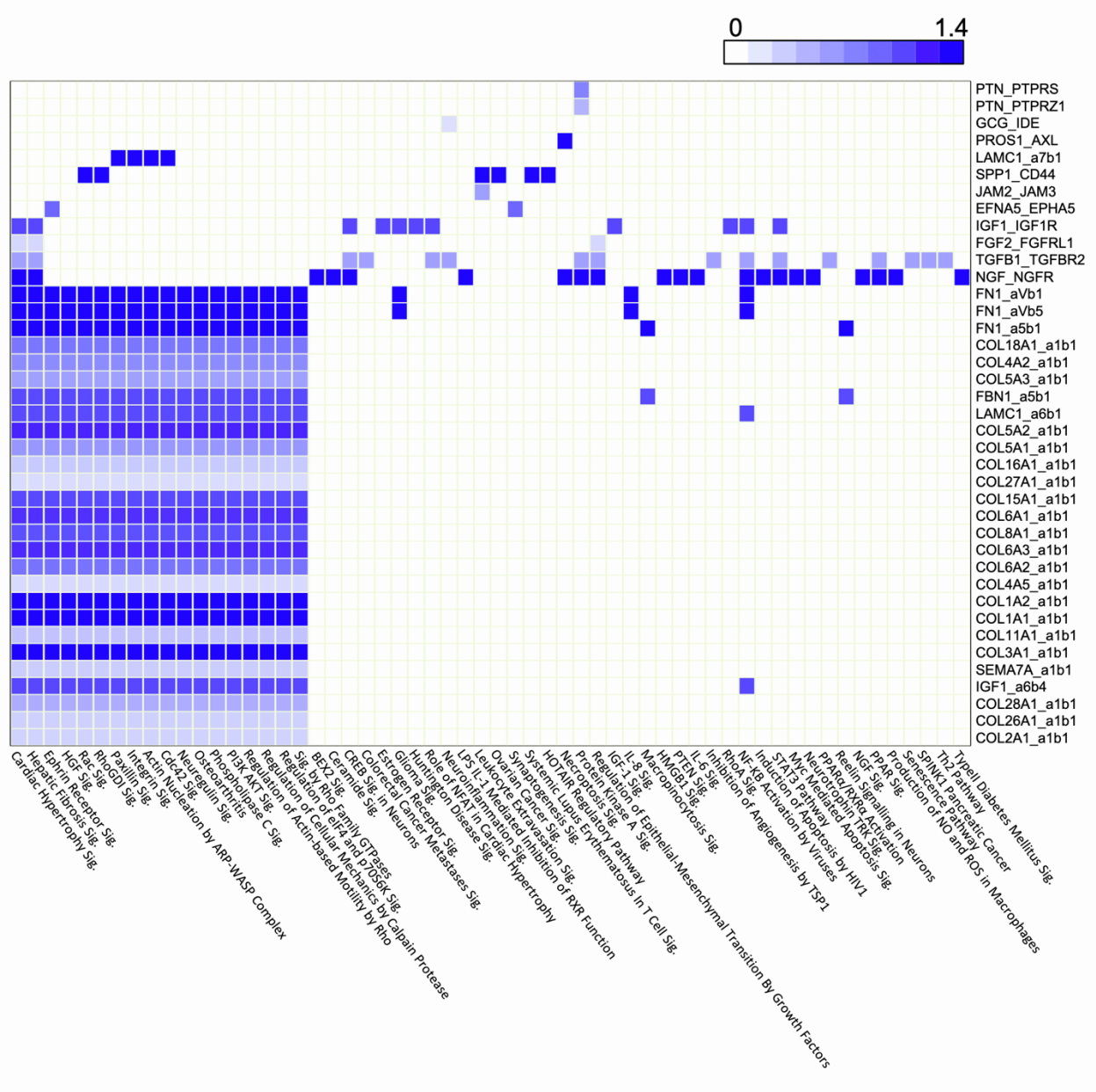

Figure S9. Integration of interactome analysis and gene ontology, Related to Figure 6

Heatmap containing the molecular pathways connected to a specific receptor-ligand pair for the interactions between glial cells and activated fibroblasts, with their interaction score in blue.

Supplementary Figure 10

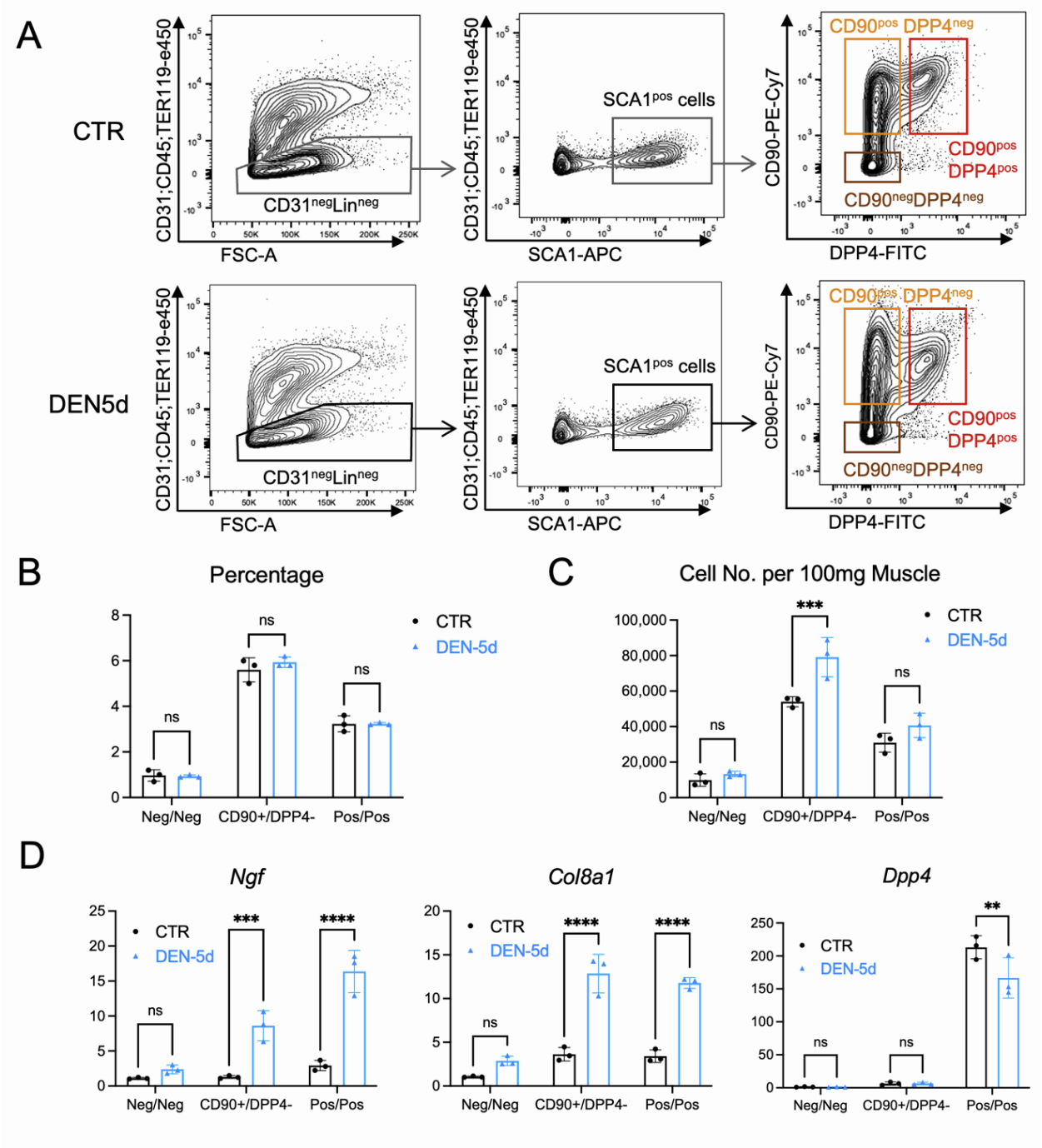

Figure S10. Sorting strategy for isolation of Activated Fibroblasts, Related to Figure 6

(A) FACS plot showing the sorting strategy for $CD90^{pos}DPP4^{neg}$ Activated Fibroblasts from muscles of Control (upper, CTR) and DEN5d (bottom) B6 mice.

(B) Percentages of $CD90^{neg}DPP4^{neg}$, $CD90^{pos}DPP4^{neg}$, $CD90^{pos}DPP4^{pos}$ cells in CTR and DEN-5d muscles.

(C) Numbers of $CD90^{neg}DPP4^{neg}$, $CD90^{pos}DPP4^{neg}$, $CD90^{pos}DPP4^{pos}$ cells in CTR and DEN-5d muscles (normalized to muscle weight).

(D) RT-qPCR results of selected genes in $CD90^{neg}DPP4^{neg}$, $CD90^{pos}DPP4^{neg}$, $CD90^{pos}DPP4^{pos}$ cells in CTR and DEN-5d muscles (normalized to *Gapdh*).

In B-D, data are represented as mean ± SD and N=3 mice.

Supplementary Figure 11

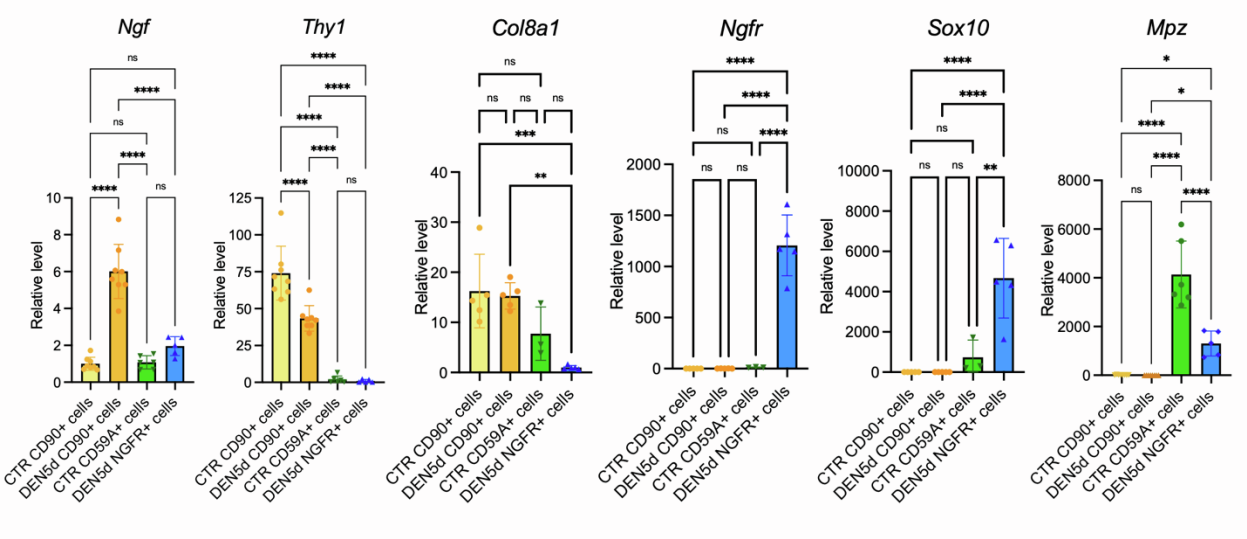

Figure S11. Validation of cell identity marker genes, Related to Figure 7

Real time PCR results of selected genes in CD90^{pos} cells, CD59A^{pos} cells, NGFR^{pos} cells isolated from CTR and DEN5d muscles (normalized to *Actb*). Statistical significance was analyzed by one-way ANOVA with P values shown as *p < 0.05, **p < 0.01, ***p < 0.001, ****p < 0.0001 and ns for not significant.

Supplementary Figure 12

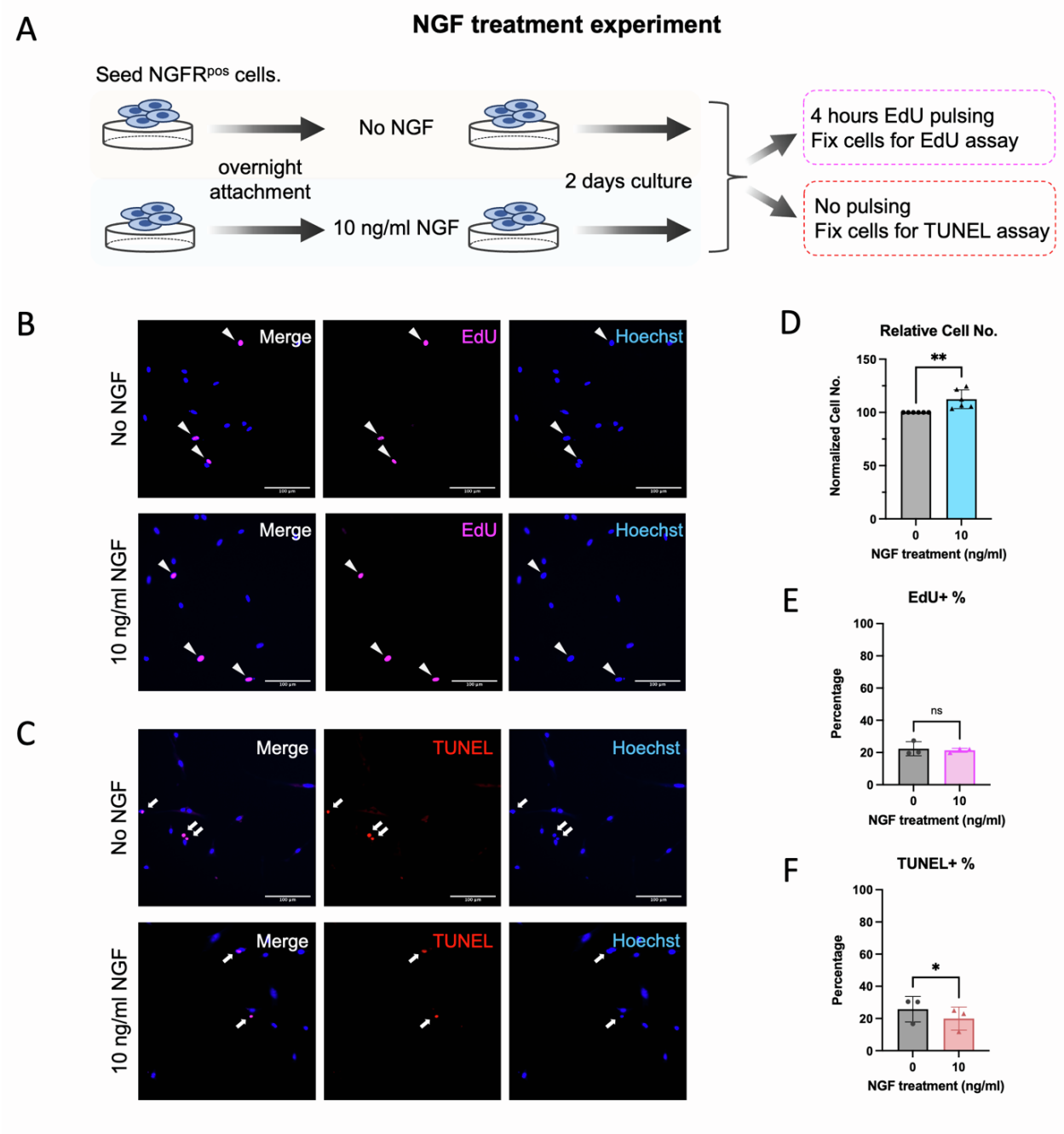

Figure S12. NGF-treatment experiment, Related to Figure 7

(A) Graphic illustration of $NGFR^{pos}$ cells with 0 or 10 ng/ml NGF treatment at Day1 to Day3 in culture. Cells were fixed for EdU assay (EdU was added for 4 hours pulsing before fixation) and TUNEL assay, respectively.

(B) Representative images of EdU staining (magenta), counterstained with Hoechst (blue). Arrow heads indicate EdU^{pos} Glial cells. Scale bar: 100μm.

(C) Representative images of TUNEL staining (red), counterstained with Hoechst (blue). Arrow heads indicate $TUNEL^{pos}$ Glial cells.

(D) Glial cell number per field was quantified in two groups. By normalization to the CTR group, relative Glial cell number was shown. N=6 mice.

(E) EdU^{pos} percentage of Glial cells with 0 or 10 ng/ml NGF treatment. N=3 mice.

(F) $TUNEL^{pos}$ percentage of Glial cells with 0 or 10 ng/ml NGF treatment. N=3 mice.

Statistical significance was analyzed by paired Student's t-test in (D-F) with P values shown as $*p < 0.05$, $**p < 0.01$, and ns for not significant.

Supplementary Table 1 Related to Figure 2A. Cell counts and percentages for each cell population per condition per replicate

Cell type	CTR_R1	CTR_R2	DEN2d_R1	DEN2d_R2	DEN5d_R1	DEN5d_R2	DEN15d_R1	DEN15d_R2
FAPs	2290 [45.3%]	2212 [40.7%]	2283 [42.6%]	2617 [47.4%]	2299 [40.8%]	1825 [39.3%]	3557 [48.4%]	2182 [40.7%]
Endothelial cells	942 [18.6%]	1173 [21.6%]	741 [13.8%]	500 [9.1%]	1182 [21%]	745 [16%]	929 [12.6%]	1017 [19%]
Tenocytes	555 [11%]	755 [13.9%]	594 [11.1%]	594 [10.8%]	660 [11.7%]	489 [10.5%]	526 [7.2%]	503 [9.4%]
MuSCs	370 [7.3%]	394 [7.2%]	472 [8.8%]	386 [7%]	363 [6.4%]	340 [7.3%]	497 [6.8%]	404 [7.5%]
Inflammatory cells	169 [3.3%]	145 [2.7%]	175 [3.3%]	285 [5.2%]	400 [7.1%]	420 [9%]	682 [9.3%]	360 [6.7%]
Myonuclei	373 [7.4%]	348 [6.4%]	529 [9.9%]	694 [12.6%]	18 [0.3%]	77 [1.7%]	27 [0.4%]	19 [0.4%]
Glial cells	40 [0.8%]	53 [1%]	158 [2.9%]	83 [1.5%]	286 [5.1%]	307 [6.6%]	376 [5.1%]	307 [5.7%]
Myotenocytes	117 [2.3%]	122 [2.2%]	100 [1.9%]	127 [2.3%]	97 [1.7%]	126 [2.7%]	420 [5.7%]	302 [5.6%]
Activated Fibroblasts	50 [1%]	72 [1.3%]	140 [2.6%]	97 [1.8%]	173 [3.1%]	188 [4%]	159 [2.2%]	117 [2.2%]
Pericytes	80 [1.6%]	107 [2%]	67 [1.3%]	60 [1.1%]	76 [1.3%]	66 [1.4%]	112 [1.5%]	108 [2%]
SMMCs	70 [1.4%]	59 [1.1%]	101 [1.9%]	77 [1.4%]	83 [1.5%]	65 [1.4%]	65 [0.9%]	44 [0.8%]
Total	**5056**	**5440**	**5360**	**5520**	**5637**	**4648**	**7350**	**5363**

Supplementary Table 2 Related to Figure 2B. Number of DE genes [UP number/ DOWN number] for each cell population at DEN2d, DEN5d, and DEN15d, respectively, in comparison with CTR.

Cell type	DEN2d [UP/DOWN]	DEN5d [UP/DOWN]	DEN15d [UP/DOWN]
FAPs	110 [59/51]	195 [115/80]	101 [70/31]
Endothelial cells	103 [63/40]	107 [64/43]	29 [14/15]
Tenocytes	100 [59/41]	115 [73/42]	46 [18/28]
MuSCs	59 [27/32]	111 [55/56]	109 [51/58]
Inflammatory cells	431 [172/259]	178 [117/61]	52 [33/19]
Myonuclei	108 [108/0]	328 [328/0]	154 [154/0]
Glial cells	1289 [923/366]	1114 [779/335]	703 [386/317]
Myotenocytes	94 [94/0]	257 [257/0]	114 [114/0]
Activated fibroblasts	862 [576/286]	564 [403/161]	442 [327/115]
Pericytes	25 [25/0]	49 [49/0]	29 [29/0]
SMMCs	82 [82/0]	51 [51/0]	36 [36/0]

Supplementary Table 3 Related to Figure 2C. Top 20 marker genes for each cell population

FAPs	Endothelial cells	Tenocytes	MuSCs	Inflamm. cells	Myonuclei	Glial cells	Myotenocytes	Activated Fibroblasts	Pericytes	SMMCs
Gsn	Fabp4	Fmod	Myod1	Cd74	Ckm	Plp1	Mb	Spp1	Rgs5	Acta2
Cxcl14	Cldn5	Thbs4	Asb5	H2-Aa	Tnnc2	Lgals3	Car3	Apod	Gm13889	Tagln
Smoc2	Aqp1	Comp	Gal	Lyz2	Tpm1	Cryab	Tpm2	Cxcl5	Ednrb	Gm13889
Col3a1	Ctla2a	Chad	Fam132b	H2-Eb1	Tnnt3	Cpe	Acta1	Ccl2	Kcnj8	Myl9
Tnfaip6	Tm4sf1	Angptl7	Sdc4	H2-Ab1	Tnni2	Btc	Mylpf	Inhba	Rgs4	Myh11
Ptx3	Isg15	Tnmd	Pmepa1	Cd14	Mylpf	Vim	Myl1	Il33	Vtn	Pmvk
Ugdh	Iigp1	Col1a1	Gpx3	C1qb	Myl1	Dbi	Tcap	Gpc3	Abcc9	Tsc22d1
Ifi205	Cxcl10	Serpinf1	Msc	Fcer1g	Acta1	Tnc	Tnni2	Tgfbi	Hopx	Mylk
Pi16	Ifit1	Cilp2	Arl4d	Cxcl2	Aldoa	Tmem158	Tnnt3	Rdh10	Art3	Mustn1
Mfap5	Flt1	Ctgf	Flnc	Tyrobp	Eno3	Ngfr	Tnnc2	Dio3	Steap4	Tpm2
Fgl2	Cdh5	Lox	Crlf1	Pf4	Actn3	Kcna1	Csrp3	Cthrc1	Rasd1	Myl6
Lum	Pecam1	Col1a2	Runx1	Cd52	Myh4	Col18a1	Slc25a4	Lif	Malat1	Pcp4l1
Cxcl1	Id1	Kera	Des	Ctss	Atp2a1	Atf3	Cox6a2	Scd1	Ebf1	Crip1
Gfpt2	Gbp2	1500015O10Rik	Cd82	C1qa	Pvalb	Ptn	Fhl1	Il11	Ndufa4l2	Rasd1
Myoc	Cd36	Timp1	Myf5	Il1b	Myoz1	Ucn2	Tpm1	Cp	Cystm1	Dstn
C3	H2-K1	Cpxm2	S100a16	Wfdc17	Gapdh	Ywhah	Atp5g1	Ccl11	Gadd45b	Flna
Has1	Plaur	Abi3bp	Pold4	Lgals3	Tcap	Gatm	Ckm	Timp1	Hspa1a	Csrp1
Ptgs2	Rsad2	Mfap4	Odc1	Ccl9	Ppp1r27	Mpz	Des	Cxcl2	Procr	Emd
Serping1	Akap12	Itgbl1	Cd63	Srgn	Slc25a4	Tubb2b	Aldoa	Lum	Hspa1b	Crem
Ccl11	Egfl7	Col12a1	Fosl1	Apoe	Pgam2	Oaf	Hspb6	Trf	Ccl11	Crispld2

Supplementary Table 4 Related to Figure S8. Top 10 EnrichR Submissions TF-Gene Co-occurrence for gene promoters containing DARs in glial cells

Term	SOX10	PLXNB3	HEYL	SOX8	FOXS1	PRRX2	HIC1	DZIP1L	HOXB2	PRRX1
Overlap	43/299	37/299	36/299	34/299	33/299	33/299	31/299	30/299	30/299	29/299
P-value	0.00	0.00	0.00	0.00	0.00	0.00	0.00	0.00	0.00	0.00
djusted P-value	0.00	0.00	0.00	0.00	0.00	0.00	0.00	0.00	0.00	0.01
Odds Ratio	3.81	3.18	3.08	2.88	2.78	2.78	2.59	2.49	2.49	2.40
ombined Score	98.67	58.06	52.61	42.74	38.30	38.30	30.35	26.82	26.82	23.56
Genes	DDR1	DDR1	SPARC	SPARC	IFITM3	IFITM3	IFITM3	SPARC	IFITM3	IFITM3
	MOXD1	CPM	COL16A1	SERPINE2	SPARC	SPARC	SPARC	COL16A1	MOXD1	SPARC
	SPARC	SPARC	SERPINE2	MEGF10	COL16A1	COL16A1	COL16A1	SERPINE2	SPARC	COL16A1
	SERPINE2	COL16A1	LPAR1	TRIL	SERPINE2	SERPINE2	SERPINE2	LPAR1	SERPINE2	SERPINE2
	TTYH2	GAL3ST1	TNC	LPAR1	ITGB3	LPAR1	ITGB3	TNC	LPAR1	LPAR1
	MEGF10	SERPINE2	ATP1A2	TNC	LPAR1	TNC	LPAR1	AEBP1	TNC	TNC
	TRIL	LPAR1	AEBP1	ATP1A2	TNC	AEBP1	TNC	FSTL1	TNFAIP2	AEBP1
	LPAR1	TNC	FSTL1	NCALD	TNFAIP2	FSTL1	TNFAIP2	LTBP1	FSTL1	FSTL1
	TNC	TGFA	LTBP1	CTGF	AEBP1	WISP1	AEBP1	NCALD	CTGF	LTBP1
	TGFA	HR	CTGF	LFNG	FSTL1	CTGF	FSTL1	CTGF	CSRP2	WISP1
	ATP1A2	CTGF	LFNG	PTPRZ1	LTBP1	CNN2	CTGF	DPYSL3	FRZB	CTGF
	NDRG2	PTPRZ1	ISLR	FRZB	WISP1	ISLR	ISLR	PLCE1	STC2	ADAMTS5
	NCALD	FCGRT	FRZB	TUBB3	CTGF	CSRP2	GPR153	IGF2BP2	DPYSL3	ISLR
	CTGF	DPYSL3	DPYSL3	APOD	ADAMTS5	FRZB	DPYSL3	IER3	TIMP1	DPYSL3
	RELN	APOD	GPC3	APOE	ISLR	STC2	EMILIN1	GSN	IER3	EMILIN1
	PTPRZ1	APOE	EMILIN1	KIF1A	EMILIN1	DPYSL3	APOE	TPM2	TFAP2A	TIMP1
	CHL1	TIMP1	APOE	IER3	TIMP1	EMILIN1	IER3	PLAUR	NR2F1	GSN
	FRZB	IER3	TIMP1	NGFR	IER3	TIMP1	NR2F1	INHBA	PLAUR	TPM2
	APOD	NGFR	VSTM4	GSN	GGT5	IER3	PLAUR	DCLK1	G0S2	INHBA
	APOE	DTNA	NGFR	NR2F1	PLAUR	GSN	G0S2	DHRS3	ISG15	DCLK1
	KIF1A	GSN	GSN	OLIG1	ISG15	TPM2	INHBA	RUNX1	INHBA	RUNX1
	RXRG	CMTM5	TPM2	S100B	INHBA	NR2F1	RUNX2	SFRP1	DHRS3	SFRP1
	TFAP2A	S100B	NR2F1	SOX10	NGF	INHBA	DHRS3	MMP14	RUNX1	MMP14
	NGFR	SOX10	INHBA	DCLK1	RUNX1	DCLK1	RUNX1	COL4A2	SFRP1	COL4A2
	GPR17	DHRS3	DCLK1	SFRP1	HEYL	RUNX1	MMP14	COL4A1	COL4A2	COL4A1
	GSN	P2RX7	DHRS3	TUBB2B	MMP14	SFRP1	COL4A2	CSPG4	COL4A1	TGFBI
	CMTM5	SFRP1	SFRP1	GAP43	COL4A2	MMP14	COL4A1	TGFBI	TGFBI	MYL9
	NR2F1	MMP14	MMP14	DAAM2	COL4A1	COL4A2	TGFBI	MYL9	MYL9	NES
	OLIG1	COL4A2	COL4A2	COL4A1	CSPG4	COL4A1	MYL9	NES	ATF3	ATF3
	S100B	DAAM2	DAAM2	MAP1B	TGFBI	CSPG4	NES	ATF3	HOXB6	
	DCLK1	QPCT	COL4A1	ADGRB1	MYL9	TGFBI	ATF3			
	RUNX1	CD9	CSPG4	CD9	NES	MYL9				
	SFRP1	CSPG4	TGFBI	NES	ATF3	ATF3				
	TUBB2B	PLXNB1	MYL9	ATF3						
	GAP43	TGFBI	NES							
	COL4A2	MYL9	ATF3							
	DAAM2	ATF3								
	COL4A1									
	CD9									
	CSPG4									
	TGFBI									
	NES									
	ATF3									

Supplementary Table 5 Related to STAR Methods Key Resource Table (Oligonucleotides section): List of real time PCR primers used in this paper.

Oligonucleotide name	Sequence (5' to 3')
Mus_Dpp4_qPCR_F1	ACCGTGGAAGGTTCTTCTGG
Mus_Dpp4_qPCR_R1	CACAAAGAGTAGGACTTGACCC
Mus_Ngf_qPCR_F1	CCAGTGAAATTAGGCTCCCTG
Mus_Ngf_qPCR_R1	CCTTGGCAAAACCTTTATTGGG
Mus_Col8a1_qPCR_F1	ACTCTGTCAGACTCATTCAGGC
Mus_Col8a1_qPCR_R1	CAAAGGCATGTGAGGGACTTG
Mus_GAPDH_qPCR_F1	CACCATCTTCCAGGAGCGAG
Mus_GAPDH_qPCR_R1	CCTTCTCCATGGTGGTGAAGAC
Mus_Actb_qPCR_F1	CACTGTCGAGTCGCGTCC
Mus_Actb_qPCR_R1	TCATCCATGGCGAACTGGTG
Mus_Thy1_qPCR_F1	TGCTCTCAGTCTTGCAGGTG
Mus_Thy1_qPCR_R1	TGGATGGAGTTATCCTTGGTGTT
Mus_Ngfr_qPCR_F1	TGCCTGGACAGTGTTACGTT
Mus_Ngfr_qPCR_R1	ACAGGGAGCGGACATACTCT
Mus_Sox10_qPCR_F1	ACACCTTGGGACACGGTTTTC
Mus_Sox10_qPCR_R1	TAGGTCTTGTTCCTCGGCCAT
Mus_Mpz_qPCR_F1	TCTCAGGTCACGCTCTATGTC
Mus_Mpz_qPCR_R1	GCCAGCAGTACCGAATCAG

Supplemental reference

[S1] Wolbert, J., Li, X., Heming, M., Mausberg, A.K., Akkermann, D., Frydrychowicz, C., Fledrich, R., Groeneweg, L., Schulz, C., Stettner, M., et al. (2020). Redefining the heterogeneity of peripheral nerve cells in health and autoimmunity. Proc Natl Acad Sci U S A *117*, 9466–9476. 10.1073/pnas.1912139117.